Multifunctional Zn-Ln (Ln = Eu and Tb) heterometallic metal-organic frameworks with highly efficient I_2 capture, dye adsorption, luminescence sensing and white light emission

Wei Gao, Han Wei, Cui-Li Wang, Jie-Ping Liu and Xiu-Mei Zhang*

Table S1. The ICP analysis results of **2-8**.

Sample	Feed molar ratio (Eu:Tb)	Measured (Eu:Tb)
$Zn_3Eu_{0.3}Tb_{1.7}$ (**2**)	0.3:1.7	0.28:1.72
$Zn_3Eu_{0.6}Tb_{1.4}$ (**3**)	0.6:1.4	0.62:1.38
$Zn_3Eu_{0.9}Tb_{1.1}$ (**4**)	0.9:1.1	0.88:1.2
$Zn_3Eu_1Tb_1$ (**5**)	1:1	1.01:0.99
$Zn_3Eu_{1.2}Tb_{0.8}$ (**6**)	1.2:0.8	1.2:0.8
$Zn_3Eu_{1.5}Tb_{0.5}$ (**7**)	1.5:0.5	1.51:0.49
$Zn_3Eu_{1.8}Tb_{0.2}$ (**8**)	1.8:0.2	1.78:0.22

Table S2 Selected bond lengths (Å) and angles (°) for Zn_3Tb_2 (**1**).

Tb1-O4	2.314(7)	Tb1-O19	2.315(6)
Tb1-O23A	2.321(5)	Tb1-O3	2.324(7)
Tb1-O22	2.390(6)	Tb1-O5	2.431(6)
Tb1-O1B	2.447(6)	Tb1-O2B	2.478(6)
Tb2-O18	2.308(6)	Tb2-O10C	2.308(5)
Tb2-O7	2.344(6)	Tb2-O9	2.350(6)
Tb2-O16	2.366(6)	Tb2-O17	2.397(7)
Tb2-O14D	2.425(6)	Tb2-O15D	2.457(6)
Zn1-O12	1.951(10)	Zn1-O13	1.957(8)
Zn1-N9	1.967(10)	Zn1-N13	1.988(9)
Zn2-O21	1.906(6)	Zn2-O24A	1.936(6)
Zn2-O20	1.942(6)	Zn2-N4E	1.988(7)
Zn3-O8	1.938(6)	Zn3-O6	1.941(7)
Zn3-O11C	1.977(6)	Zn3-N19E	2.010(8)
O4-Tb1-O19	96.4(3)	O4-Tb1-O23A	157.9(2)
O19-Tb1-O23A	91.9(2)	O4-Tb1-O3	83.5(3)
O19-Tb1-O3	147.7(3)	O23A-Tb1-O3	100.2(3)

O4-Tb1-O22	80.7(2)	O19-Tb1-O22	73.5(2)
O23A-Tb1-O22	82.1(2)	O3-Tb1-O22	137.5(2)
O4-Tb1-O5	83.0(3)	O19-Tb1-O5	141.5(2)
O23A-Tb1-O5	77.8(2)	O3-Tb1-O5	70.7(3)
O22-Tb1-O5	68.4(2)	O4-Tb1-O1B	129.2(2)
O19-Tb1-O1B	75.4(2)	O23A-Tb1-O1B	72.8(2)
O3-Tb1-O1B	79.8(3)	O22-Tb1-O1B	138.9(2)
O5-Tb1-O1B	133.4(2)	O4-Tb1-O2B	77.0(2)
O19-Tb1-O2B	73.3(2)	O23A-Tb1-O2B	125.1(2)
O3-Tb1-O2B	75.3(2)	O22-Tb1-O2B	137.2(2)
O5-Tb1-O2B	142.1(2)	O1B-Tb1-O2B	52.3(2)
O18-Tb2-O10C	155.7(2)	O18-Tb2-O7	103.3(3)
O10C-Tb2-O7	89.2(2)	O18-Tb2-O9	83.4(2)
O10C-Tb2-O9	80.9(2)	O7-Tb2-O9	71.7(2)
O18-Tb2-O16	91.6(3)	O10C-Tb2-O16	89.4(2)
O18-Tb2-O17	81.0(3)	O10C-Tb2-O17	76.6(2)
O7-Tb2-O17	142.3(2)	O9-Tb2-O17	71.7(2)
O16-Tb2-O17	70.0(3)	O18-Tb2-O14D	76.4(2)
O10C-Tb2-O14D	127.5(2)	O7-Tb2-O14D	73.9(2)
O9-Tb2-O14D	134.4(2)	O16-Tb2-O14D	80.0(2)
O17-Tb2-O14D	141.6(2)	O18-Tb2-O15D	128.9(2)
O10C-Tb2-O15D	74.3(2)	O7-Tb2-O15D	74.0(2)
O9-Tb2-O15D	137.6(2)	O16-Tb2-O15D	72.4(2)
O17-Tb2-O15D	132.1(2)	O14D-Tb2-O15D	53.4(2)
O12-Zn1-O13	100.0(4)	O12-Zn1-N9	117.8(4)
O13-Zn1-N9	105.4(4)	O12-Zn1-N13	106.5(4)
O13-Zn1-N13	111.8(4)	N9-Zn1-N13	114.3(4)
O21-Zn2-O24A	120.6(3)	O21-Zn2-O20	113.8(3)
O24A-Zn2-O20	112.1(3)	O21-Zn2-N4E	99.1(3)
O24A-Zn2-N4E	107.4(3)	O20-Zn2-N4E	100.5(3)
O8-Zn3-O6	108.4(3)	O8-Zn3-O11C	132.0(3)
O6-Zn3-O11C	109.0(3)	O8-Zn3-N19E	103.4(3)
O6-Zn3-N19E	103.3(3)	O11C-Zn3-N19E	96.2(3)

Symmetry codes: A: x-1/2, -y+3/2, -z+1; B: x-1, y, z; C:x+1/2, -y+3/2, -z+2; D: x+1, y, z; E: -x+1, y-1/2, -z+3/2.

Table S3 Selected bond lengths (Å) and angles (°) for Zn_3Eu_2 (**9**).

Eu1-O19	2.336(6)	Eu1-O4	2.337(6)
Eu1-O23A	2.339(5)	Eu1-O3	2.349(6)
Eu1-O22	2.406(5)	Eu1-O5	2.448(6)
Eu1-O1B	2.466(6)	Eu1-O2B	2.494(5)
Eu2-O10C	2.328(5)	Eu2-O18	2.334(6)
Eu2-O7	2.367(6)	Eu2-O9	2.375(5)
Eu2-O16	2.389(5)	Eu2-O17	2.416(7)

Eu2-O14D	2.449(6)	Eu2-O15D	2.472(5)
Zn1-O12	1.944(8)	Zn1-O13	1.951(8)
Zn1-N9	1.965(8)	Zn1-N13	1.969(8)
Zn2-O21	1.910(6)	Zn2-O24A	1.938(6)
Zn2-O20	1.944(6)	Zn2-N4E	2.001(6)
Zn3-O6	1.940(6)	Zn3-O8	1.948(5)
Zn3-O11C	1.978(5)	Zn3-N19E	2.011(7)
O19-Eu1-O4	96.9(2)	O19-Eu1-O23A	91.1(2)
O4-Eu1-O23A	157.9(2)	O19-Eu1-O3	148.0(2)
O4-Eu1-O3	83.4(3)	O23A-Eu1-O3	100.5(2)
O19-Eu1-O22	73.27(19)	O4-Eu1-O22	81.0(2)
O23A-Eu1-O22	81.63(19)	O3-Eu1-O22	137.7(2)
O19-Eu1-O5	141.3(2)	O4-Eu1-O5	70.7(2)
O23A-Eu1-O5	77.8(2)	O3-Eu1-O5	70.7(2)
O22-Eu1-O5	68.5(2)	O19-Eu1-O1B	75.0(2)
O4-Eu1-O1B	128.9(2)	O23A-Eu1-O1B	73.1(2)
O3-Eu1-O1B	80.0(2)	O22-Eu1-O1B	138.6(2)
O5-Eu1-O1B	133.6(2)	O19-Eu1-O2B	73.27(19)
O4-Eu1-O2B	77.3(2)	O23A-Eu1-O2B	124.79(19)
O3-Eu1-O2B	75.6(2)	O22-Eu1-O2B	137.21(18)
O5-Eu1-O2B	142.6(2)	O1B-Eu1-O2B	51.85(19)
O10C-Eu2-O18	156.1(2)	O10C-Eu2-O7	88.6(2)
O18-Eu2-O7	103.3(2)	O10C-Eu2-O9	80.0(2)
O18-Eu2-O9	84.2(2)	O7-Eu2-O9	71.3(2)
O10C-Eu2-O16	89.0(2)	O18-Eu2-O16	92.2(3)
O7-Eu2-O16	146.0(2)	O9-Eu2-O16	141.2(2)
O10C-Eu2-O17	76.7(2)	O18-Eu2-O17	81.2(3)
O7-Eu2-O17	141.8(2)	O9-Eu2-O17	71.5(2)
O16-Eu2-O17	69.8(2)	O10C-Eu2-O14D	127.36(18)
O18-Eu2-O14D	76.3(2)	O7-Eu2-O14D	74.4(2)
O9-Eu2-O14D	135.1(2)	O16-Eu2-O14D	80.3(2)
O17-Eu2-O14D	141.7(2)	O10C-Eu2-O15D	74.54(19)
O18-Eu2-O15D	128.4(2)	O7-Eu2-O15D	74.6(2)
O9-Eu2-O15D	137.5(2)	O16-Eu2-O15D	72.1(2)
O17-Eu2-O15D	132.1(2)	O14D-Eu2-O15D	53.05(18)
O12-Zn1-O13	100.5(4)	O12-Zn1-N9	118.4(4)
O13-Zn1-N9	104.8(4)	O12-Zn1-N13	106.5(4)
O13-Zn1-N13	112.0(4)	N9-Zn1-N13	113.9(4)
O21-Zn2-O24A	121.3(2)	O21-Zn2-O20	113.4(3)
O24A-Zn2-O20	112.3(3)	O21-Zn2-N4E	99.2(2)
O24A-Zn2-N4E	106.9(3)	O20-Zn2-N4E	100.2(3)
O6-Zn3-O8	108.5(3)	O6-Zn3-O11C	109.2(3)
O8-Zn3-O11C	132.5(2)	O6-Zn3-N19E	103.0(3)

O8-Zn3-N19E	103.0(2)	O11C-Zn3-N19E	95.7(3)

Symmetry codes: A: x+1/2, -y+1/2, -z+1; B: x+1, y, z; C: x-1/2, -y+1/2, -z; D: x-1, y, z; E: -x+1, y+1/2, z+1/2.

Table S4. CIE color coordinate of $Zn_3Eu_xTb_{2-x}$ (**1-9**).

λ=298 nm	CIE coordinate	
$Zn_3Eu_xTb_{2-x}$ (**1-9**)	x	y
Zn_3Tb_2 (**1**)	0.27	0.46
$Zn_3Eu_{0.3}Tb_{1.7}$ (**2**)	0.28	0.45
$Zn_3Eu_{0.6}Tb_{1.4}$ (**3**)	0.30	0.44
$Zn_3Eu_{0.9}Tb_{1.1}$ (**4**)	0.29	0.38
Zn_3EuTb_1 (**5**)	0.31	0.37
$Zn_3Eu_{1.2}Tb_{0.8}$ (**6**)	0.31	0.35
$Zn_3Eu_{1.5}Tb_{0.5}$ (**7**)	0.33	0.33
$Zn_3Eu_{1.8}Tb_{0.2}$ (**8**)	0.35	0.28
Zn_3Eu_2 (**9**)	0.36	0.24

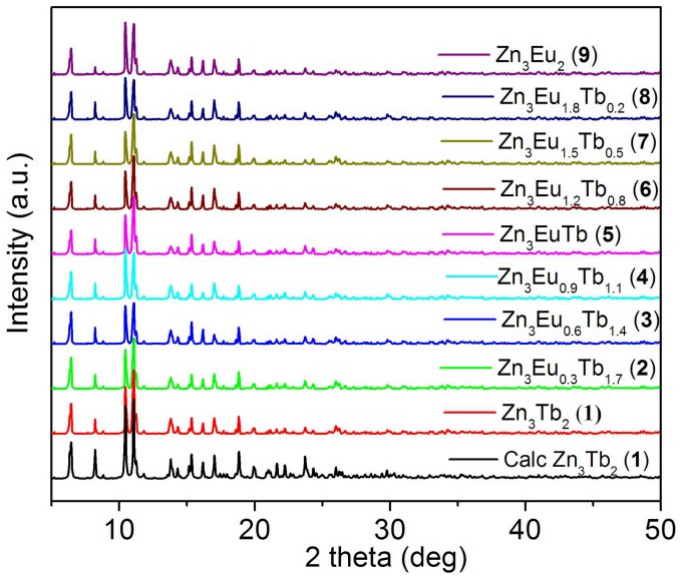

Fig. S1 PXRD patterns of $Zn_3Eu_xTb_{2-x}$ **(1-9)** (black line) simulated from the single-crystal data, (other color lines) for the as-synthesized sample.

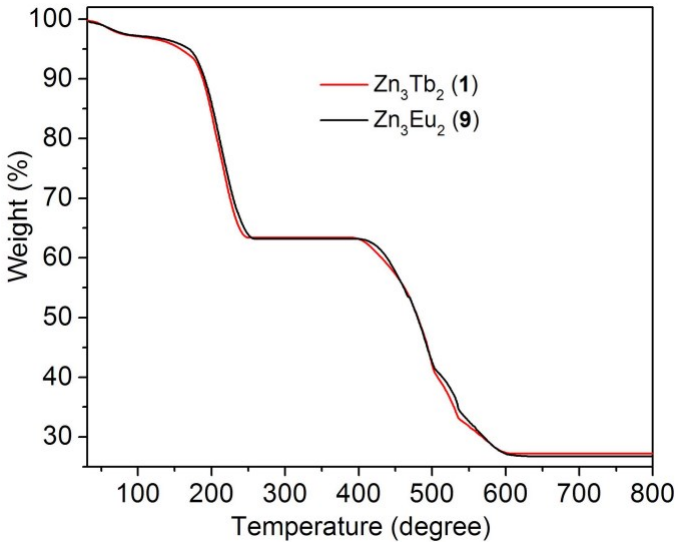

Fig. S2 TGA plots of Zn_3Tb_2 (**1**) and Zn_3Eu_2 (**9**) under air environment.

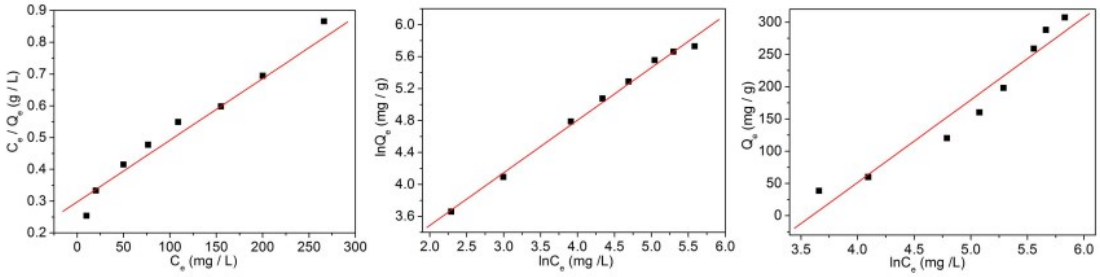

Fig. S3 Plots of the fitting of the I_2 adsorption on Zn_3Tb_2 (**1**) experimental data with Langmuir isotherm (left), Freundlich (middle) and Themkin isotherm models (right).

Table S5 Parameters of the adsorption of I_2 on Zn_3Tb_2 (**1**).

Models	Parameters	I_2
Langmuir	q_m (mg·g^{-1})	515.46
	b (L·mg^{-1})	0.0065
	R^2	0.9817
Freundlich	n	1.49
	kF (mg·g^{-1}(L·mg^{-1})$^{1/n}$)	8.356
	R^2	0.996
Tempkin	A (L·g^{-1})	0.023
	B	127.85
	R^2	0.9708

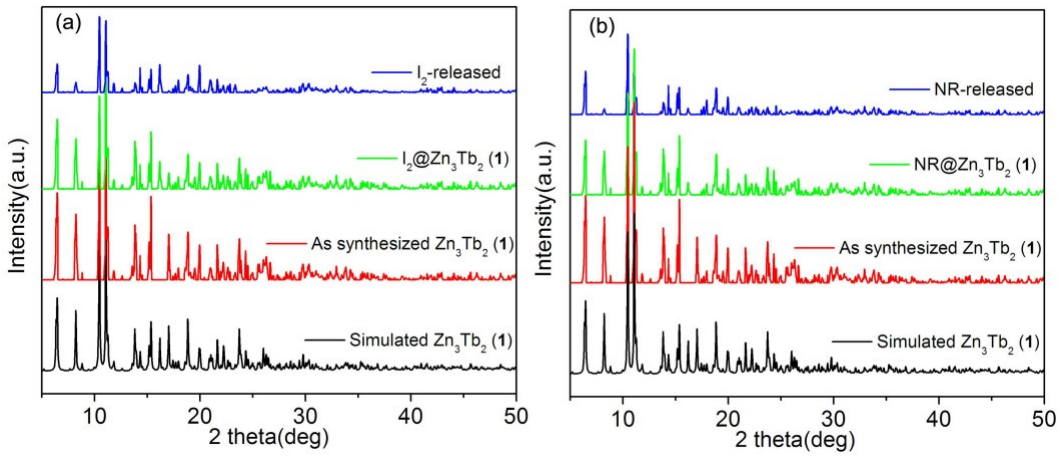

Fig. S4 The PXRD patterns of Zn_3Tb_2 (**1**) after the absorption and desorption of I_2 (a) and NR (b).

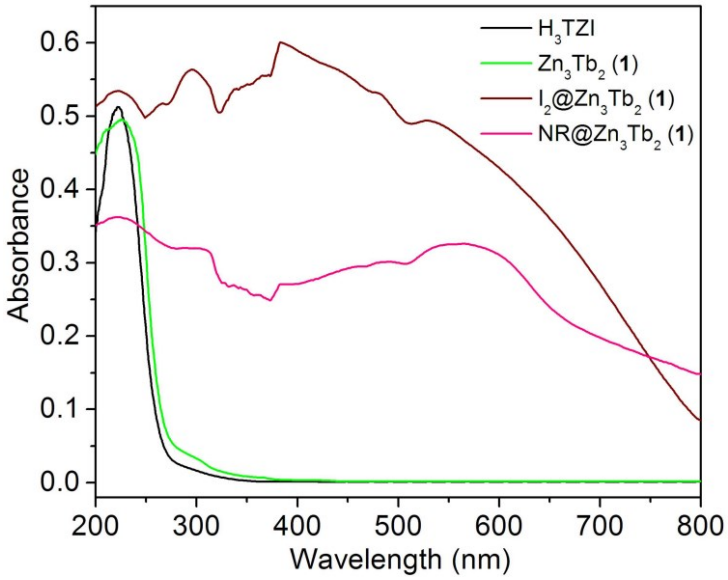

Fig. S5 Solid-state UV-vis spectra of free H_3TZI ligand, Zn_3Tb_2 (**1**), iodine-loaded samples and NR-loaded samples.

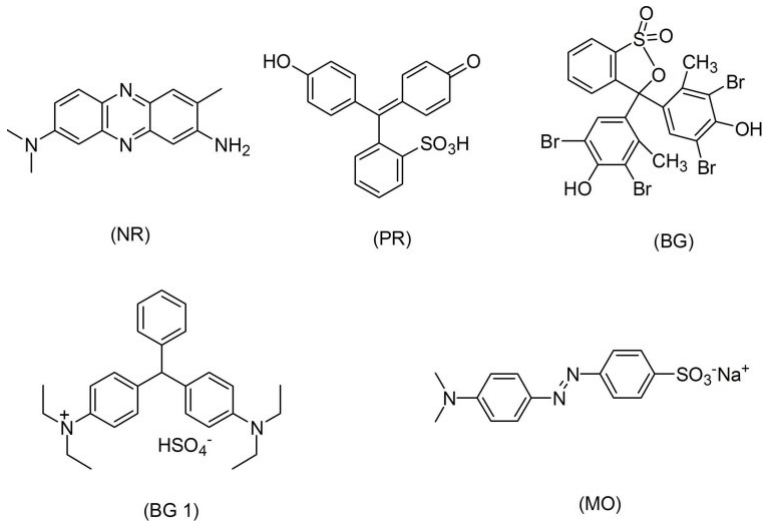

Fig. S6 The structures of the selected dye molecules.

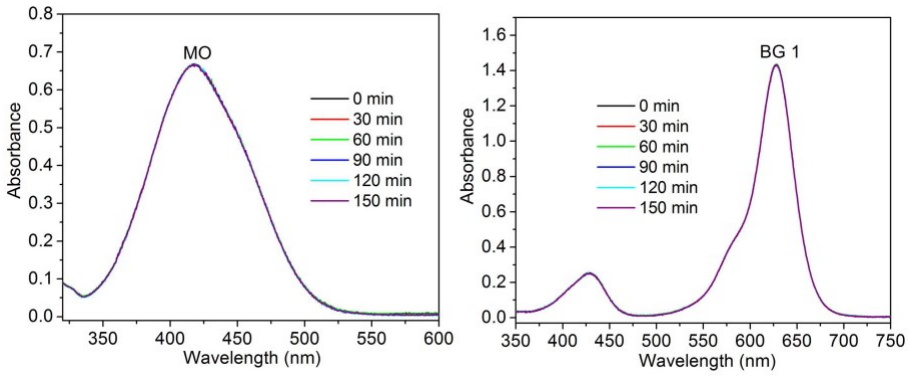

Fig. S7 UV-vis spectra of EtOH solutions of MO and BG 1 in the presence of Zn_3Tb_2 (**1**) with time.

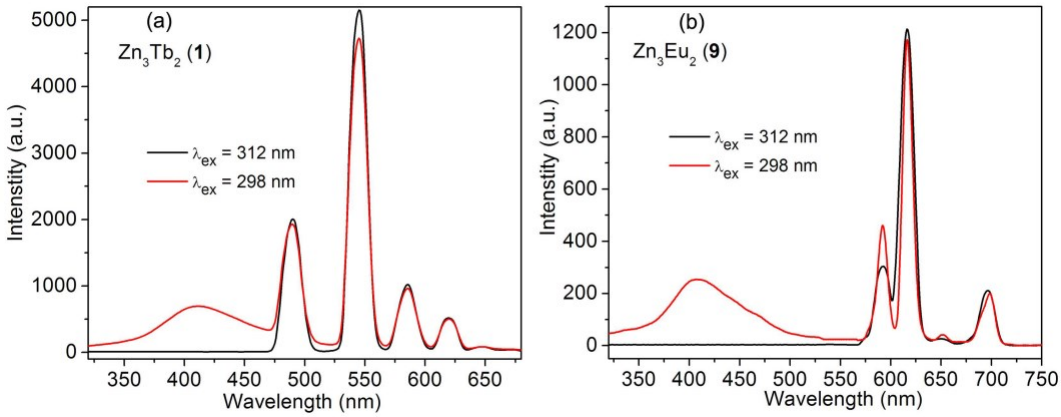

Fig. S8 Solid state emission spectra of Zn_3Tb_2 (**1**) (a) and Zn_3Eu_2 (**9**) (b) at room temperature.

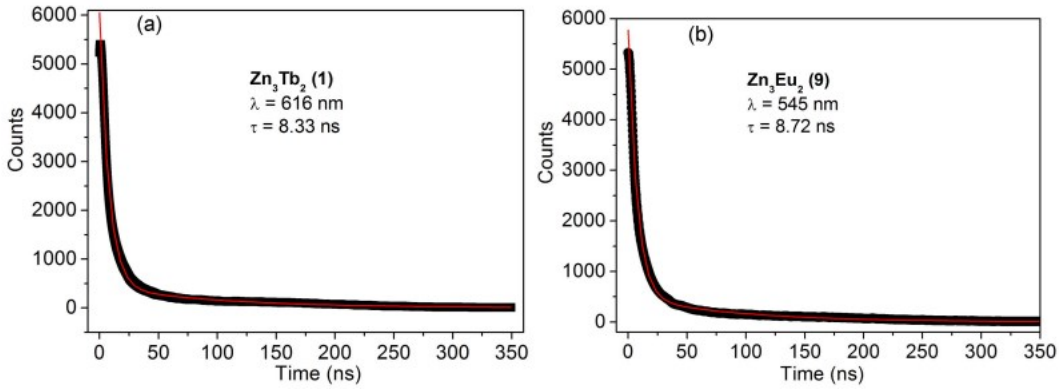

Fig. S9 Decay curves and luminescence lifetime of Zn_3Tb_2 (**1**) (a) and Zn_3Eu_2 (**9**).

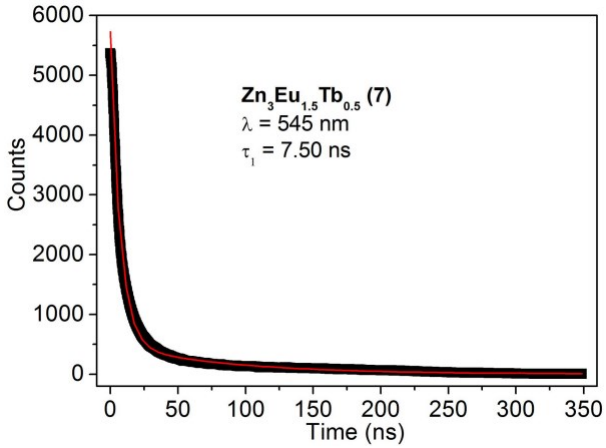

Fig. S10 Decay curves and luminescence lifetime of $Zn_3Eu_{1.5}Tb_{0.5}$ (**7**).

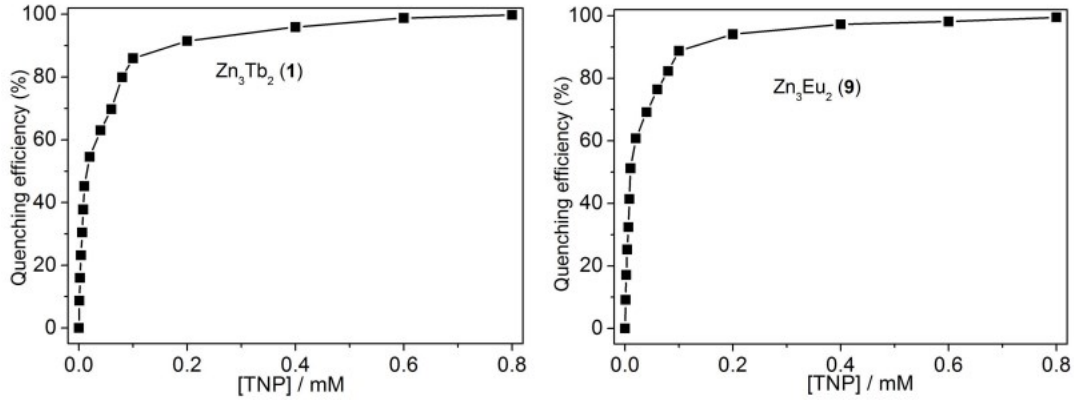

Fig. S11 Dependence of the quenching efficiency on the concentration of TNP.

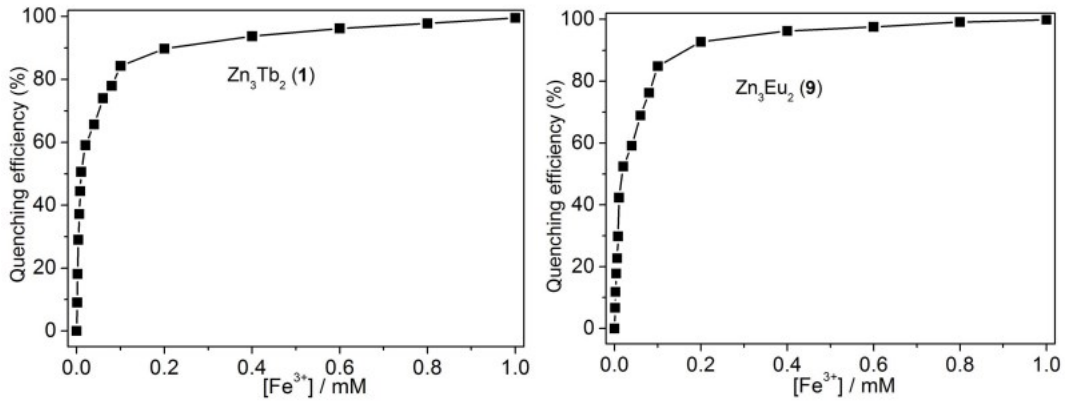

Fig. S12 Dependence of the quenching efficiency on the concentration of Fe^{3+} ions.

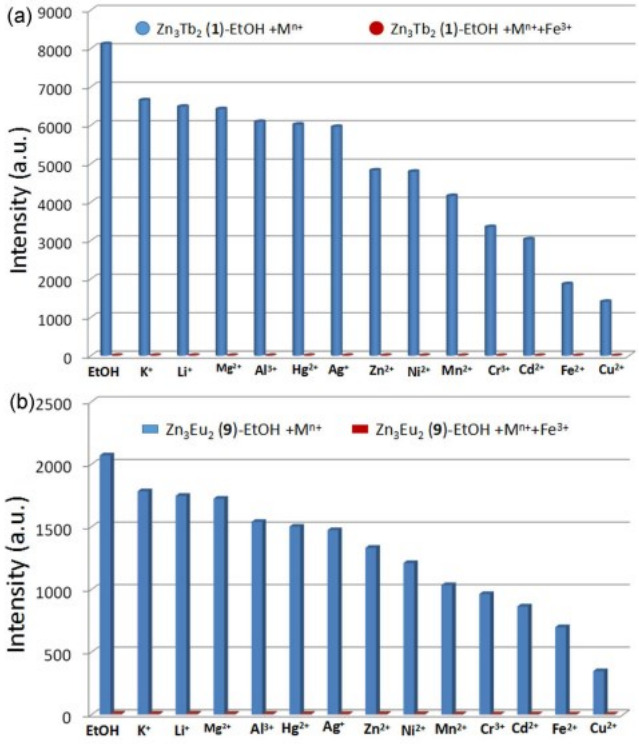

Fig. S13 The luminescent intensity of Zn_3Tb_2 (**1**) (a) and Zn_3Eu_2 (**9**) (b) on Fe^{3+} sensing.

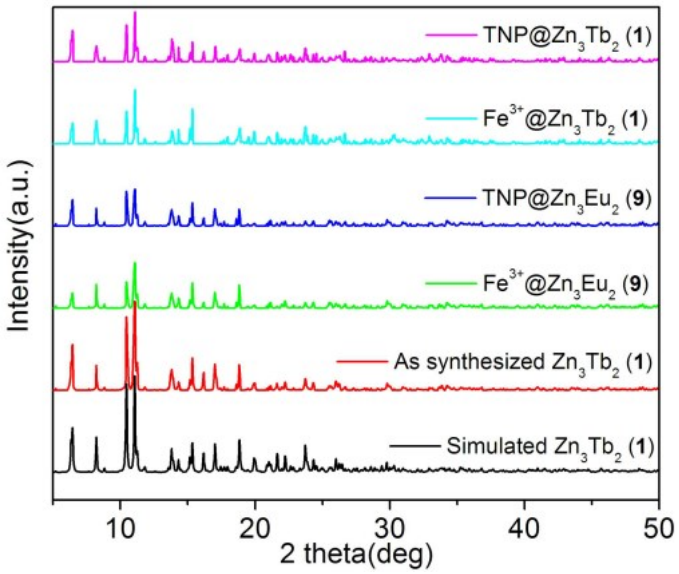

Fig. S14 PXRD patterns of Zn_3Tb_2 (**1**) and Zn_3Eu_2 (**9**) immersed in TNP and Fe^{3+} solution.

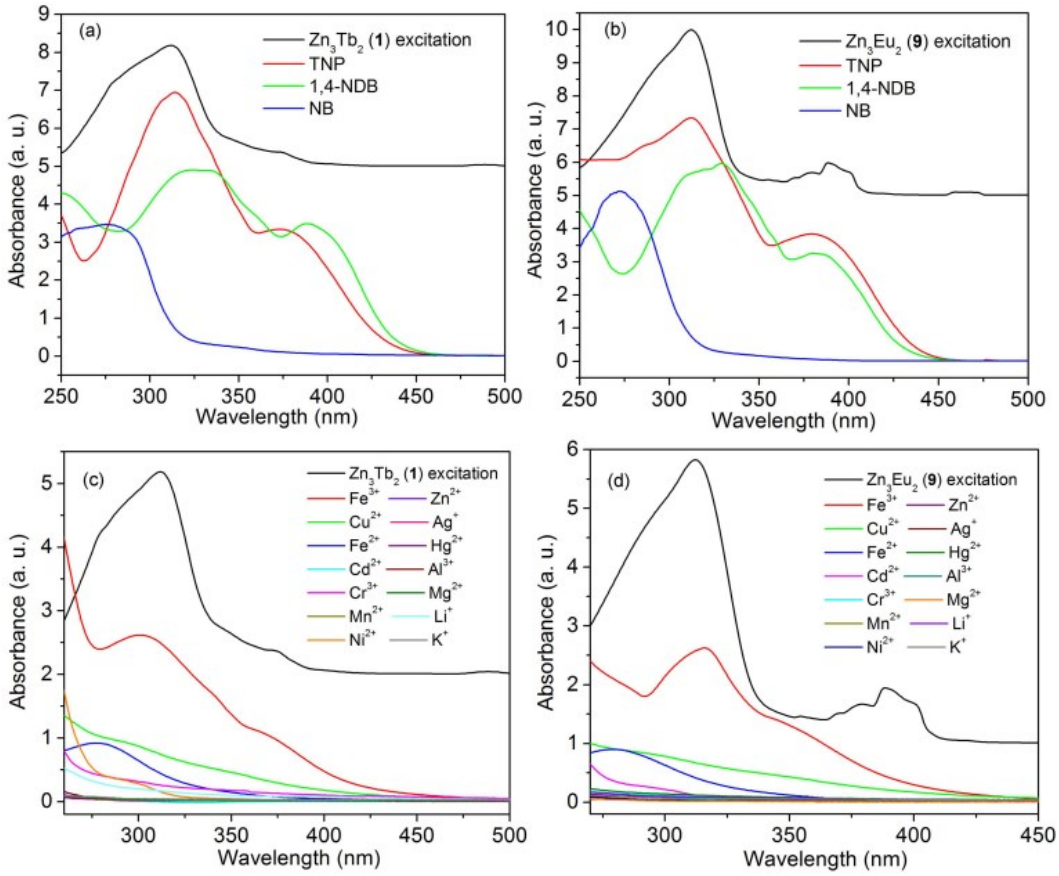

Fig. S15 UV-vis adsorption spectrum of TNP, 1,4-NDB, NB and $M(NO_3)_x$ EtOH solutions and the excitation spectrum of Zn_3Tb_2 (**1**) (a, c) and Zn_3Eu_2 (**9**) (b, d).

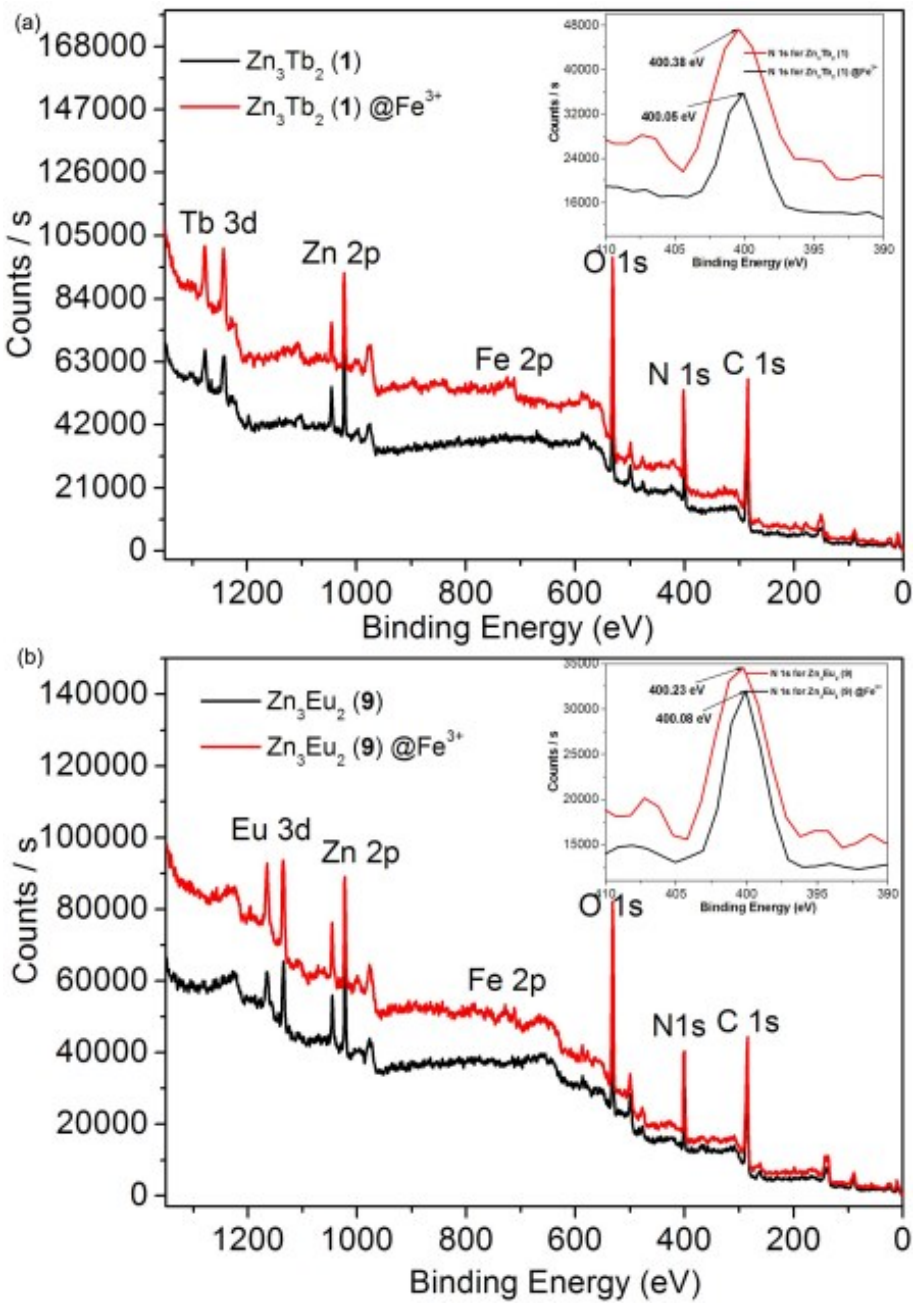

Fig. S16 Comparison of the XPS spectra of Zn_3Tb_2 (**1**) (a) and Zn_3Eu_2 (**9**) (b) before and after treatment with Fe^{3+} ions. Inset: picture showing the spectra of N 1s.